Lateral structure of uniform flow

Robert J. Sobey

ABSTRACT

The concept of uniform flow is traditionally associated with a cross-section-integrated description of channel flow. In some analyses of flow in wide channels, it may be appropriate to adopt a depth-integrated description. The ensuing lateral structure of the depth-integrated flow is investigated at uniform flow. The steady state ordinary differential equation for the lateral structure is established, along with the formulation as a boundary value problem. An integral part of the formulation is the relationship between the channel resistance models for cross-section-integrated and depth-integrated descriptions, respectively. Predictions are shown for a rectangular channel and for an irregular channel.

Key words | uniform flow, natural channels, lateral profile, eddy viscosity

Rodney J. Sobey
Department of Civil and Environmental Engineering,
Imperial College London,
London SW7 2AZ,
UK
E-mail: *r.j.sobey@imperial.ac.uk*

INTRODUCTION

Uniform flow in a channel is a flow state that is rarely experienced but it is nonetheless influential in characterizing channel flows. In particular, it has a fundamental role in characterizing channel friction. The familiar channel resistance closure models, Chèzy, Darcy–Weisbach and Manning, are uniform flow formulae. In steady gradually varied flow, uniform flow is the asymptotic state. In unsteady flow, steady gradually varied flow is the local time-averaged flow.

The traditional analysis of uniform flow is based on a cross-section-integrated description of channel flow. The flow is characterized by the cross-section-integrated flow Q and the water surface elevation η. Channel resistance is characterized by a constant cross-section-averaged friction factor, C, f or n, depending on the closure model. At uniform flow, Q, the flow cross-section A and the water surface slope $\partial\eta/\partial x$ are all constant. There is no prediction of flow structure within the cross section.

A depth-integrated description of channel flow provides some flow structure. The flow is characterized by depth-integrated flows q_x in the longitudinal direction and q_y in the lateral direction, together with the water surface elevation η. The conservation equations must now include mass and momentum fluxes in both the longitudinal and lateral directions. The vector momentum equations must also include lateral momentum transfer, without which there would be slip at lateral boundaries and no lateral boundary layer structure. Channel resistance is here characterized by a bottom friction factor (C or f or n) to represent shear in the vertical and an eddy viscosity ε to represent shear in the horizontal. Together, the bottom friction factor and the horizontal eddy viscosity assume the role of the cross-section-averaged friction factor in the cross-section-integrated description.

A depth-integrated description provides the opportunity to predict the lateral flow structure at uniform flow. As context, this paper will initially review the traditional cross-section-integrated prediction of uniform flow conditions in a natural channel. It will then consider the definition of uniform flow conditions with a depth-integrated description of channel flow. An ordinary differential equation is established to describe the lateral flow structure $q_x(y)$ at uniform flow. The associated boundary value problem is formulated, and solved numerically. An integral part of the analysis is the relationship between the cross-section-integrated friction factor and the combination of bottom friction factor and horizontal eddy

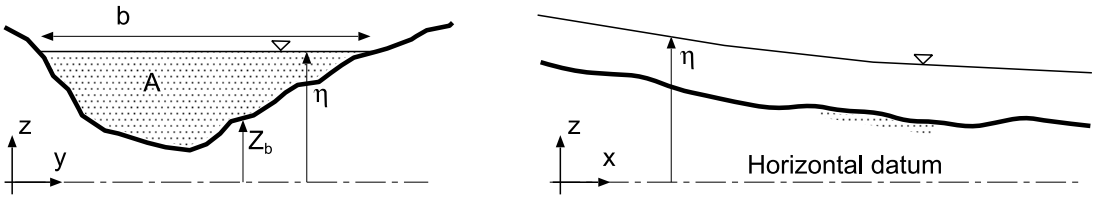

Figure 1 | Definition sketch for narrow channel.

viscosity. Illustrative predictions are provided for a rectangular and a natural channel.

CROSS-SECTION-INTEGRATED DESCRIPTION

Most analyses of nearly horizontal flow in natural channels adopt a cross-section-integrated description (see Figure 1). The independent variables are longitudinal position x and time t, the dependent variables are $\eta(x,t)$ the local water surface elevation to a fixed horizontal datum and $Q(x,t)$ the local discharge or cross-section-integrated flow.

The cross-section-integrated conservation equations are

$$b\frac{\partial \eta}{\partial t}+\frac{\partial Q}{\partial x}=0$$
$$\frac{\partial Q}{\partial t}+\frac{\partial}{\partial x}\left(\frac{Q^2}{A}\right)=-gA\frac{\partial \eta}{\partial x}-\frac{\tau_0}{\rho}P \quad (1)$$

in which $A(x,t)$ is the local flow cross section, $P(x,t)$ is the local wetted perimeter,

$$A=\int_A (\eta-z_b)dy,\ \ P=\int_{\text{Bed}}\sqrt{1+\left(\frac{dz_b}{dy}\right)^2}\,dy \quad (2)$$

$z_b(x,y)$ is the local bed elevation, $b(x,t)$ is the local surface width, g is the gravitational acceleration and $\tau_0(x,t)$ is the boundary shear. The quadratic Darcy–Weisbach friction model is adopted, with

$$\tau_0=\frac{f}{8}\rho\frac{|Q|Q}{A^2} \quad (3)$$

in which f is the Darcy–Weisbach friction factor. The alternative Chèzy or Manning models can be substituted without any fundamental change in the analysis. These details are given subsequently.

The special case of steady flow has received considerable attention in open channel flow. Omitting the time-dependent terms, the long wave equations reduce to the gradually varied flow equations:

$$Q=\text{constant}$$
$$\frac{d}{dx}\left(\frac{Q^2}{A}\right)=-gA\frac{d\eta}{dx}-\frac{f}{8}\frac{|Q|Q}{A^2}P \quad (4)$$

which describe the steady-state flow on which flood and tidal flows are imposed (Henderson 1966). For uniform flow, dA/dx is zero, so that $d\eta/dx$ $(=dz_b/dx=-S_0)$, A and P are also constant, and

$$0=gAS_0-\frac{f}{8}\frac{Q^2}{A^2}P. \quad (5)$$

For a flat-bottom channel (rectangular, trapezoidal, etc), a uniform $(\eta-z_b)_n=d_n$ depth (the normal depth) can be established by solution of implicit algebraic Equation (5). But note that this requires the additional assumption that the lateral water surface profile is horizontal.

For a natural channel, the depth varies across the channel and the concept of a normal depth is not especially satisfactory. But the concept of uniform flow remains appropriate. It would be more useful to

characterize uniform flow by the cross-section area at uniform flow, the normal area A_n. A_n might be estimated implicitly from Equation (5). But again there is the additional assumption that the lateral water surface profile is horizontal in the identification of the local elevation of the water surface and also in the identification of the lateral locations of both the left and right banks.

The lateral structure of the water surface and the lateral location of the left and right banks are issues that are directly addressed in the following consideration of a depth-integrated description of uniform flow. The cross-section-integrated description precludes any prediction of the lateral (cross-stream) structure of η, Q and d_n or A_n.

DEPTH-INTEGRATED DESCRIPTION

The lateral flow structure of nearly horizontal flow in natural channels is retained by including the lateral position y along with the longitudinal position x and time t as the independent variables. The dependent variables become water surface elevation $\eta(x,y,t)$ and the depth-integrated flows

$$q_x(x,y,t)=\int_{-h}^{\eta} u_x dz, \quad q_y(x,y,t)=\int_{-h}^{\eta} u_y dz \tag{6}$$

in which the bed elevation is at $z_b=-h(x,y)$ in common practice, and (u_x,u_y) are the local velocity components. The depth-integrated mass and momentum conservation are

$$\frac{\partial \eta}{\partial t}+\frac{\partial q_x}{\partial x}+\frac{\partial q_y}{\partial y}=0 \tag{7}$$

$$\begin{aligned}&\frac{\partial q_x}{\partial t}+\frac{\partial}{\partial x}\left(\frac{q_x^2}{h+\eta}\right)+\frac{\partial}{\partial y}\left(\frac{q_x q_y}{h+\eta}\right)=-g(h+\eta)\frac{\partial \eta}{\partial x}+2\frac{\partial}{\partial x}\left(\varepsilon\frac{\partial q_x}{\partial x}\right)\\&+\frac{\partial}{\partial y}\left(\varepsilon\left[\frac{\partial q_x}{\partial y}+\frac{\partial q_y}{\partial x}\right]\right)-\frac{f'}{8}\frac{|q|q_x}{(h+\eta)^2}\\&\frac{\partial q_y}{\partial t}+\frac{\partial}{\partial x}\left(\frac{q_x q_y}{h+\eta}\right)+\frac{\partial}{\partial y}\left(\frac{q_y^2}{h+\eta}\right)=-g(h+\eta)\frac{\partial \eta}{\partial y}\\&+\frac{\partial}{\partial x}\left(\varepsilon\left[\frac{\partial q_x}{\partial y}+\frac{\partial q_y}{\partial x}\right]\right)+2\frac{\partial}{\partial y}\left(\varepsilon\frac{\partial q_y}{\partial y}\right)-\frac{f'}{8}\frac{|q|q_y}{(h+\eta)^2}\end{aligned} \tag{8, 9}$$

from which both Coriolis accelerations and surface wind stresses have been omitted. The friction model becomes

$$\tau_{0\alpha}=\frac{f'}{8}\rho\frac{|q|q_\alpha}{(h+\eta)^2}, \ \alpha=x,y \tag{10}$$

locally, in which the Darcy–Weisbach friction factor f' for this depth-integrated description is consistent (but not identical; see Equation (17)) with the f for the cross-section-integrated model (Equation (3)).

Lateral momentum transfer has been modelled as

$$\frac{\partial}{\partial x_\beta}\int_{-h}^{\eta}(\bar{\tau}_{\alpha\beta}-\overline{\rho u'_\alpha u'_\beta})\,dz=\frac{\partial}{\partial x_\beta}\left(\rho\varepsilon\left[\frac{\partial q_\beta}{\partial x_\alpha}+\frac{\partial q_\alpha}{\partial x_\beta}\right]\right) \tag{11}$$

by analogy with the general form of Newton's law of viscosity; $\bar{\tau}_{\alpha\beta}$ and $\overline{\rho u'_\alpha u'_\beta}$ are the local viscous and Reynolds stresses in the horizontal plane and ε is the horizontal eddy viscosity. In the cross-section-integrated description, both vertical and horizontal momentum transfer are scaled by a constant f. In the depth-integrated description, vertical momentum transfer is scaled by f' and horizontal momentum transfer is scaled by ε. Consistent with the practice in cross-section-integrated descriptions, both f' and ε are assumed constant in the depth-integrated description.

The integral parameter Q is

$$Q=\int_A q_x dy \tag{12}$$

where A was defined in Equation (2), except for the sign change convention in the representation of the bed elevation.

A definition of uniform flow for depth-integrated descriptions of channel flow that is consistent with Equation (5) for a cross-section-integrated description would have

(i) steady flow, $\frac{\partial \eta}{\partial t}=\frac{\partial q_x}{\partial t}e=\frac{\partial q_y}{\partial t}=0$

(ii) no longitudinal variation in flow, $\frac{\partial q_x}{\partial x}=\frac{\partial q_y}{\partial x}=0$, and

(iii) constant channel resistance parameters f' and ε.

Equation (7) together with no flow boundary boundary conditions at the channel sides gives $q_y \equiv 0$. Equation (9) gives $\partial\eta/\partial y = 0$, so that $\eta = \eta(x)$, a function of x only. The residual terms in Equation (8) become

$$0=-g(h+\eta)\frac{\partial \eta}{\partial x}+\varepsilon\frac{\partial^2 q_x}{\partial y^2}-\frac{f'}{8(h+\eta)^2}|q_x|q_x \tag{13}$$

or

$$\varepsilon\frac{d^2 q_x}{dy^2}+gd_nS_0-\frac{f'q_x^2}{8d_n^2}=0 \tag{14}$$

in which both $d_n = (h + \eta)$ and q_x are functions of y. Given $d_n(y)$, Equation (14) is a second-order ordinary differential equation for the lateral velocity profile $q_x(y)$. It is in the familiar form of a boundary layer equation, requiring no slip at the banks and describing the lateral diffusion of boundary shear from the banks.

Suitable boundary conditions on Equation (14) are no flow at y_L, the left hand channel bank and at y_R, the right hand channel bank:

$$q_x(y_L) = 0 \; q_x(y_R) = 0 \tag{15}$$

together with the integral condition

$$Q=\int_{y_L}^{y_R} q_x(y)dy \tag{16}$$

that identifies the cross-section-integrated discharge Q. Q is a given parameter.

The relationship between the cross-section-integrated friction factor f, the depth-integrated friction factor f' and the horizontal eddy viscosity ε is established from Equations (5) and (14). Integrating (14) over the cross section and comparing terms gives

$$-gAS_0=-\frac{f'}{8}\frac{Q^2}{A^2}P=\varepsilon\frac{dq_x}{dy}\Big|_{y_L}^{y_R}-\frac{f'}{8}\int_{y_L}^{y_R}\left(\frac{q_x}{h+\eta}\right)^2 dy. \tag{17}$$

The place of f' and ε in the depth-integrated description is taken by f alone in the cross-section-integrated description. Equation (17) is, in fact, two equations, relating the constant water surface slope to cross-section-integrated and to depth-integrated descriptions of the channel resistance, respectively.

NUMERICAL ALGORITHM

Stage 1

For a natural channel, the depth varies across the channel, but the water surface elevation remains horizontal across the channel. The flow cross section at uniform flow can be characterized by the elevation $\Delta\eta$ of the water surface (or equivalently by the flow cross section). Equation (17a) (or (5)) becomes the implicit algebraic equation

$$f(\Delta\eta)=gAS_0-\frac{f}{8}\frac{Q^2}{A^2}P \tag{18}$$

with A and P defined as in Equation (2) but with $z_b = -h$. A number of numerical algorithms (bisection, Newton–Raphson, secant method, etc) are suitable for implicit algebraic equations in a single unknown.

Numerical precision that is consistent with the balance of the subsequent discussion of depth-integrated flow is achieved by computing A and P from the ordinary differential equations

$$\frac{dY_1}{dy}=h+\Delta\eta$$
$$\frac{dY_2}{dy}=\sqrt{1+\left(\frac{dh}{dy}\right)^2} \tag{19}$$

in which dY_1/dy is dA/dy and dY_2/dy is dP/dy. Both h and dh/dy are required as continuous functions of y. Bathymetry specified as discrete (y_i,h_i) pairs is anticipated,

with cubic spline interpolation providing smooth and continuous estimates for h and dh/dy as required. Bathymetric resolution must be adequate to follow the significant detail of the cross section. Inadequate resolution will not be improved by the spline interpolation.

Initial conditions are $Y_1 = Y_2 = 0$ at $y = y_L$. Integration from y_L to y_R gives $A = Y_1(y_R)$ and $P = Y_2(y_R)$. Excellent precision is achieved with an error-correcting, adaptive step size (mixed fourth- and fifth-order Runge–Kutta) code for numerical integration.

Estimation of y_L and y_R is formulated as the implicit algebraic equation

$$f_{L,R}(y) = 0 = h(y) + \Delta\eta. \tag{20}$$

Given $\Delta\eta$ and the bathymetry $h(y)$, there are two solutions to Equation (20), respectively y_L at the left bank and y_R at the right bank. Equations (20) may be solved by the same numerical algorithm adopted for Equation (18).

This Stage 1 algorithm requires knowledge of the channel geometry, together with the assigned Q, S_0 and f. A successful numerical solution provides $\Delta\eta$, y_L, y_R, A and P.

Stage 2

The lateral boundary layer Equation (14) is equivalent to the simultaneous first-order ODE system:

$$\frac{dZ_1}{dy} = \frac{Z_2}{\varepsilon}$$
$$\frac{dZ_2}{dy} = -gd_nS_0 + \frac{f'Z_1^2}{8d_n^2} \tag{21}$$

where Z_1 is q_x and Z_2 is $\varepsilon dq_x/dy$. But numerical integration of Equations (21) requires initial conditions at a known y on both Z_1 and Z_2. $Z_1(y_L) = 0$, but $Z_2(y_L) = \zeta$ is unknown. The second boundary condition is $Z_1(y_R) = 0$. Locally, $d_n(y) = h(y) + \Delta\eta$, in which $\Delta\eta$ is known from Stage 1.

The problem is formulated as the simultaneous implicit algebraic equations

$$f_1(\zeta,\varepsilon,f') = 0 = q_x(y_R)$$
$$f_2(\zeta,\varepsilon,f') = 0 = \int_{y_L}^{y_R} q_x(y)dy - Q$$
$$f_3(\zeta,\varepsilon,f') = 0 = gAS_0 + (Z_2(y_R) - \zeta) - \frac{f'}{8}\int_{y_L}^{y_R}\left(\frac{q_x(y)}{h(y)+\Delta\eta}\right)dy. \tag{22}$$

This system is nonlinear through Equation (21b), which is involved in the definition of Equation (22b, c). Evaluation of $Z_1(y_R)$ and $Z_2(y_R)$ requires numerical integration of Equations (21) with initial conditions $Z_1 = 0$ and $Z_2 = z$ at y_L; z is an unknown. As the integrals in Equations (22b, c) must also be evaluated numerically, consistent numerics is assured by redefining the ODE system as

$$\frac{dZ_1}{dy} = \frac{Z_2}{\varepsilon}$$
$$\frac{dZ_2}{dy} = -g(h+\eta)S_0 + \frac{fZ_1^2}{8(h+\Delta\eta)^2}$$
$$\frac{dZ_3}{dy} = Z_1$$
$$\frac{dZ_4}{dy} = \frac{Z_1^2}{(h+\eta)^2} \tag{23}$$

where

$$Z_3 = \int_{y_L}^{y} q_x dy - Q \quad \textit{and} \quad Z_4 = \int_{y_L}^{y} \frac{q_x^2}{(h+\Delta\eta)^2}\,dy \tag{24}$$

with initial conditions $Z_1 = 0$, $Z_2 = \zeta$, $Z_3 = -Q$ and $Z_4 = 0$ at y_L. The simultaneous implicit algebraic equations become

$$f_1(\zeta,\varepsilon,f') = 0 = Z_1(y_R)$$
$$f_2(\zeta,\varepsilon,f') = 0 = Z_3(y_R)$$
$$f_1(\zeta,\varepsilon,f') = 0 = gAS_0 + (Z_2(y_R) - \zeta) - \frac{f'}{8}Z_4(y_R). \tag{25}$$

Newton's method (Press *et al.* 1992) is a suitable choice for the numerical solution of Equations (25), with a error-correcting adaptive step size Runge–Kutta code as

before for the numerical integration of Equations (23). An error-correcting adaptive step size ODE code ensures adequate precision in evaluations of Equations (25). As the evaluation of the implicit Equations (25) involves the numerical integration of the ordinary differential equations (23), numerical precision in the evaluation of Equations (25) becomes a potentially significant issue. The use of IEEE standard double (64 bit) precision is important; this is now implicit in many engineering software platforms.

It is also recognized that the definition of Z_2 to Z_4 in Equations (23) makes it very likely that Z_1 to Z_4 will be very different in magnitude, as they also are in dimensions. Possible numerical precision consequences have been avoided by non-dimensionalizing all variables by a space scale that approximates the width W of the channel, and a timescale $W/\overline{U}$, where $\overline{U}$ approximates the mean flow velocity in the channel.

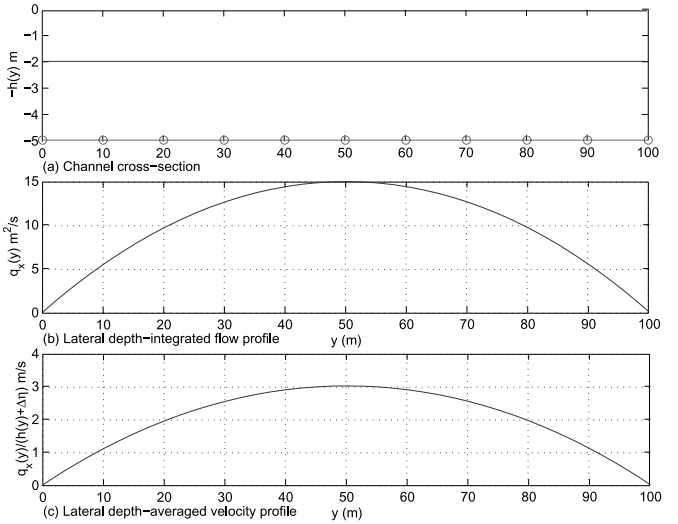

Figure 2 | Rectangular channel.

CHANNEL FRICTION

The bottom friction factors f and f' and the horizontal eddy viscosity ε are independent parameters in the numerical algorithm. Their physical relationship is established through Equation (17).

The cross-section-integrated friction factor f is a given parameter. The expected magnitude of the depth-integrated friction factor f' would be of the order of f but rather smaller in magnitude, as resistance in the depth-integrated description is contributed by both f' and ε.

A simple order-of-magnitude estimate for the horizontal eddy viscosity is provided by a zero equation turbulence model, in which

$$\varepsilon \approx u_* l \tag{26}$$

where u_* is the velocity scale of the turbulence and l is the length scale of the turbulence.

The velocity scale of the turbulence is the shear velocity $u_* = \sqrt{(\tau_b/\rho)}$. From the cross-section-integrated Darcy–Weisbach friction model, the boundary shear is $\tau_b = (f/8)\rho\overline{U}^2$, where the cross-section-averaged flow velocity $\overline{U}$ is $Q/(Wd)$. W is the channel width and d is the mean channel depth.

The length scale of the turbulence would be the large eddy scale, for which the mean channel depth d is a good estimate.

Using these estimates for the velocity and length scales of the turbulence, an order-of-magnitude estimate for the horizontal eddy viscosity is

$$\varepsilon \approx \left(\frac{f}{8}\right)^{1/2} \frac{Q}{W}. \tag{27}$$

This is a suitable initial estimate for ε in Equations (25).

APPLICATION

As an initial example, consider a rectangular channel (Figure 2(a)) of width 100 m and local bed at elevation -5 m. The markers in Figure 2(a) show the discrete (y_i, h_i) bathymetry pairs that communicate the channel bathymetry. The bed slope S_0 is 0.001, the friction factor f is 0.02 and the cross-section-integrated flow Q is 1000 m^3/sec.

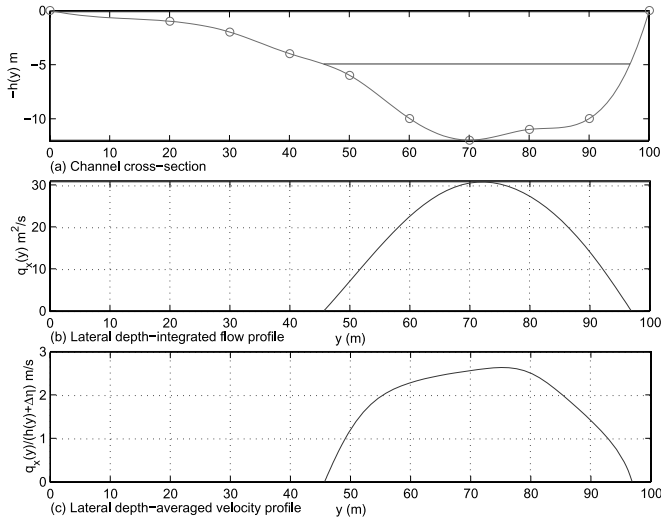

Figure 3 | Natural channel.

From the Stage 1 algorithm, $\Delta\eta = -2.00$ m, $y_L = 0$ m, $y_R = 100$ m and $A = 300.0$ m^2. From the Stage 2 algorithm, $\varepsilon = 2.26$ m^2/sec and $f' = 0.0011$. Figure 2(b) shows the $q_x(y)$ profile. The profile is symmetric, as expected. The near-bank gradients are significantly less steep than those that would characterize a turbulent boundary layer between parallel plates. But this is a lateral profile of a depth-integrated flow, where the depth integration has integrated over the boundary layer profile in the vertical. The mean flow velocity gradients near the bed would be quite sharp. Figure 2(c) shows the equivalent lateral profile of $q_x(y)/[h(y) + \Delta\eta]$, the depth-averaged velocity.

Figure 3(a) is a natural channel of roughly similar width and cross-section area. The same S_0, f and Q as for the rectangular channel example are adopted.

From the Stage 1 algorithm, $\Delta\eta = -4.95$ m, $y_L = 45.65$ m, $y_R = 96.79$ m and $A = 240.0$ m^2. From the Stage 2 algorithm, $\varepsilon = 0.55$ m^2/sec and $f' = 0.0021$. Figure 3(b) shows the $q_x(y)$ profile, and Figure 3(c) the $q_x(y)/[h(y) + \Delta\eta]$ profile. As a direct consequence of the irregular bathymetry, the lateral flow profile is asymmetric.

A further application of such structured uniform flow solutions would be in the prediction of the longitudinal dispersion coefficient for contaminant transport in the same channel. The Taylor–Elder–Fischer theory (Fischer *et al.* 1979) requires knowledge of the lateral distribution of the depth-integrated flow together with the horizontal coefficient of turbulent momentum diffusion. This information is provided by the present theory.

CHÈZY AND MANNING FRICTION MODELS

Chèzy model

The relationship between C and f is direct:

$$f = \frac{8g}{\varepsilon^2} \quad or \quad \varepsilon = \sqrt{\frac{8g}{f}}. \tag{28}$$

As f is dimensionless, the simplest approach would be to retain the previous algorithm, with a prior translation from C to f and a subsequent translation from f' to C′.

Manning model

The changes are more fundamental for the Manning model. The cross-section-integrated n would be specified in place of f and a depth-integrated n' predicted in place of f'. SI units are assumed in the following discussion. For FSS (foot–second–slug) units, n and n' are replaced by $n/1.49$ and $n'/1.49$, respectively.

Equation (14) becomes

$$\varepsilon\frac{d^2q_x}{dy^2} + gd_nS_0 - gn'^2\frac{q_x^2}{d_n^{7/3}} = 0 \tag{29}$$

and Equation (17) becomes

$$-gAS_0 = -gn^2\frac{Q^2}{A^{7/3}}P^{4/3} = \varepsilon\frac{dq_x}{dy}\Big|_{y_L}^{y_R} - gn'^2\int_{y_L}^{y_R}\frac{q_x^2}{(h+\eta)^{7/3}}\,dy. \tag{30}$$

In Stage 1 of the algorithm, Equation (18) would become

$$f(\Delta\eta) = gAS_0 - gn^2\frac{Q^2}{A^{7/3}}P^{4/3}. \tag{31}$$

In Stage 2 of the algorithm, Equation (23) becomes

$$\frac{dZ_1}{dy}=\frac{Z_2}{\varepsilon}$$

$$\frac{dZ_2}{dy}=g(h+\Delta\eta)S_0+gn'^2\frac{Z_1^2}{(h+\Delta\eta)^{7/3}}$$

$$\frac{dZ_3}{dy}=Z_1$$

$$\frac{dZ_4}{dy}=\frac{Z_1^2}{(h+\Delta\eta)^{7/3}} \tag{32}$$

and Equation (25) becomes

$$f_1(\zeta,\varepsilon,n')=0=Z_1(y_R)$$

$$f_2(\zeta,\varepsilon,n')=0=Z_3(y_R)$$

$$f_3(\zeta,\varepsilon,n')=0=gAS_0+(Z_2(y_R)-\zeta)-gn'^2Z_4(y_R). \tag{33}$$

The details are otherwise identical.

CONCLUSIONS

An analysis of the lateral structure at uniform flow in a channel has been based on the depth-integrated long wave equations. At uniform flow, it is shown that the cross-stream depth-integrated flow q_y is identically zero and that the lateral profile of the water surface is horizontal.

The lateral distribution of the streamwise depth-integrated flow q_x is shown to follow a boundary-layer-style equation, where the lateral structure responds to shear diffusion from the channel sides.

Uniform flow is described by the channel discharge Q, the bed slope S_0 and the channel (cross-section-integrated) friction factor f. Channel bathymetry is specified as (y_i,h_i) observation pairs. A two-stage numerical algorithm is formulated to solve for the cross-section area A, the left y_L and right y_R bank locations, the $q_x(y)$ profile, the horizontal eddy viscosity ε and the depth-integrated bottom friction factor f'.

Application of the algorithm to a rectangular channel and a natural channel are given. The predictions are shown to be physically plausible.

Algorithm variations for alternative channel friction models are given.

ACKNOWLEDGEMENTS

The research described and the results presented herein, unless otherwise noted, were obtained from research funded through the Scour Holes at Inlet Structures work unit of the Coastal Inlets Research Program at the US Army Engineer Research and Development Center, Coastal and Hydraulics Laboratory (CHL). Permission was granted by Headquarters, US Army Corps of Engineers, to publish this information.

REFERENCES

Fischer, H. B., List, J. L., Brooks, N. H., Imberger, J. I. & Koh, R. C. Y. 1979. *Mixing in Inland and Coastal Waters*. Academic, New York.

Henderson, F. M. 1966. *Open Channel Flow*. MacMillan, New York.

Press, W. H., Teukolsky, S. A., Vetterling, W. T. & Flannery, B. P. 1992. *Numerical Recipes in FORTRAN: The Art of Scientific Computing*, 2nd edn. Cambridge University Press, Cambridge.